

# Phase Noise Impact on BER in Space Communication

Ondrej Baran, Miroslav Kasal, Petr Vagner and Tomas Urbanec

**Abstract**—This paper deals with the modeling and the evaluation of a multiplicative phase noise influence on the bit error ratio in a general space communication system. Our research is focused on systems with multi-state phase shift keying modulation techniques and it turns out, that the phase noise significantly affects the bit error rate, especially for higher signal to noise ratios. These results come from a system model created in Matlab environment and are shown in a form of constellation diagrams and bit error rate dependencies. The change of a user data bit rate is also considered and included into simulation results. Obtained outcomes confirm theoretical presumptions.

**Keywords**—Additive thermal noise, AWGN, BER, bit error rate, multiplicative phase noise, phase shift keying.

## I. INTRODUCTION

NOISE is a ubiquitous factor negatively influencing the useful signal transmission in every communication system. In the area of extraterrestrial communication systems (satellite as well as deep space) the matter of noise is much more severe than in the case of terrestrial ones. A link budget has to be properly calculated to secure the connection quality with a respect to the adequate power of the satellite. Since almost all today's communication systems are digital, the measure of signal transmission quality is expressed by an error probability, as a bit error ratio BER. In extraterrestrial narrowband low-rate communications (e.g. a low-rate satellite telemetry transmission), the most suitable modulation technique, fulfilling the requirement for the best BER achieved with the lowest necessary signal power, is a generic multi-state phase shift keying M-PSK.

Previous studies [1] confirmed that two most important noise types have to be counted with during a modeling and a design of narrowband systems. The first one is the additive thermal noise that affects the useful signal only on the receiver side of the system. The second noise type is the multiplicative phase noise that is produced in all system oscillators, i.e. in the transmitter as well as in the receiver.

An estimation of BER of a system with certain parameters is very important task during system design that can be accomplished analytically or by modeling. Computer modeling is very easy way of testing system parameters. But in a case of noise, to cover its statistical characters and its impact on BER [1], a very long useful data sequence has to be used in simulations. This puts extreme demands on computational

resources and the simulation time. Knowledge of statistical characteristics of noise processes would enable to derive BER relations analytically or semi-analytically, which would make BER estimations much easier and quicker during the system design.

General analytical expressions for BER estimations of M-PSK systems distorted only by the additive thermal noise are known. Authors in [2] – [5] propose exact formulas for BER calculations. They come from simple two-state BPSK modulation and consequently, they extend results for multi-state M-PSK cases. As an additive thermal noise, the additive white Gaussian noise process is expected. User data is coded according to the Gray bit coding.

To our knowledge, there is no technical paper describing deeper insight into problems connected with the simultaneous influence of the additive and the multiplicative noise on BER in general M-PSK systems. The aim of this paper is to investigate how the multiplicative phase noise affects the error probability in a comparison with the individual influence of the additive thermal noise. Following paragraphs describe ways of noise modeling, the simulation model of a narrowband communication system and its results used for the evaluation of BER. Simulation outcomes are concluded in the end.

## II. DESCRIPTION OF THE MODEL

For modeling purposes, very complex parts of real systems are simplified. An attention is predominantly dedicated to the noise investigation, thus system blocks that do not have a significant influence on the noise are idealized in the model. Despite these treatments, obtained results do not lose the general validity and the model can be easily modified and extended.

### A. M-PSK System Model

In a case of narrowband extraterrestrial systems, useful signals are usually transmitted in microwave frequency bands. To fulfill the sampling theorem [6], extreme sampling rates should be used to process the microwave frequencies directly. To significantly reduce the necessary sampling frequency and to enable solving these kinds of problems on computers, the baseband processing of passband signals is utilized with a help of analytical signals and complex envelopes. In this case, the sampling frequency  $f_{sam}$  has to be at least two times higher than the maximum frequency in a baseband complex envelope signal. Stating  $f_b$  as a data signal bit rate, the sampling frequency  $f_{sam}$  can be expressed according to the relation  $f_{sam} \geq 2 \cdot m \cdot f_b$ , where the integer multiple  $m$  shows how wide is the simulation bandwidth, i.e. from  $-f_{sam}/2$  to  $f_{sam}/2$ . It was determined that the minimal value of  $m$  is 3 to obtain the

O. Baran, M. Kasal, P. Vagner and T. Urbanec are with the Department of Radio Electronics, Faculty of Electrical Engineering and Communication, Brno University of Technology, Purkynova 118, 612 00 Brno, Czech Republic (e-mails: baran@feec.vutbr.cz, kasal@feec.vutbr.cz, vagner@feec.vutbr.cz, urbanec@feec.vutbr.cz).

proper signal expression in the simulator [7].

The transmission chain is divided into in-phase I and quadrature Q branches, which directly enables the modeling of signals modulated with multi-state phase shift keying M-PSK without any significant modifications. If only two-state BPSK is used, a useful signal in a quadrature branch is zero.

Fig. 1 shows the model of a general M-PSK system. The signal processing is divided into three parts – processing in a transmitter, in a transmission channel and in a receiver.

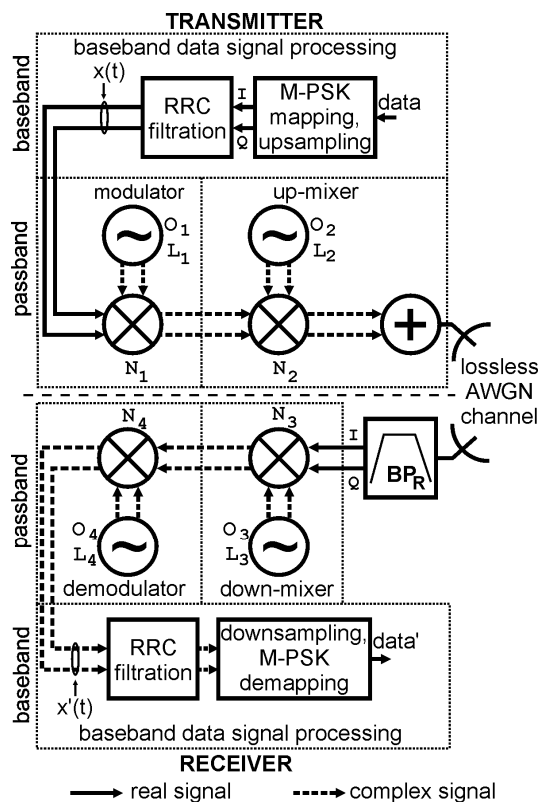


Fig. 1 A block diagram of the M-PSK system model

In the transmitter, a digital baseband data stream is Gray coded and mapped into I-Q M-PSK symbols flowing with a symbol rate  $f_s$ , i.e. one symbol per one sample. Consequently, symbols are upsampled with respect to the sampling frequency  $f_{sam}$ . The following operation is low-pass filtration in a Root-Raised Cosine (RRC) filter that performs spectrum limitations and secures the minimization of intersymbol interferences. Last operations in the transmitter are a M-PSK modulation to the high frequency carrier and an up-mixing to the microwave frequency band. The modulation and the mixing are performed in multipliers  $N_1$  and  $N_2$  and, since the processing is done in the baseband, only complex envelopes of useful signals and signals of oscillators are multiplied with each other. The only noise sources in the transmitter model are two oscillators producing the multiplicative phase noise. The additive thermal noise is not significant in the transmitter, because its level is always negligible comparing to the useful signal level.

The transmission channel forms the next part of the system model. For a simplification, it is a lossless channel with

additive thermal noise that is directly added to the useful transmitted signal.

On the receiver side, the signal goes through the band-pass filter that picks only the useful band. Consequently, it is down converted and demodulated. A receiver RRC filter together with the transmitter RRC filter serve as a matched filter maximizing the signal to noise ratio of the received signal. The following step is the downsampling with a respect to the sampling frequency, which gives one symbol per one sample. Finally, I-Q symbols are demapped back to the received data bit stream with a bit rate  $f_b$ . The down-mixing and the demodulation are performed by a multiplication (in  $N_3$  a  $N_4$ ) of baseband complex envelopes. The only noise sources in the receiver model are two oscillators producing the multiplicative phase noise. The additive thermal noise of the receiver is recalculated to the input of the receiver antenna [8] and is included in the additive thermal noise of the transmission channel.

The receiver band-pass filter  $BP_R$  is modeled as an equivalent low-pass FIR filter, which arises from the baseband processing. This opportunity also enables omitting band-pass filters following after M-PSK modulation, up-mixing and down-mixing stages. It is supposed that these filters are modeled as ideal rectangular filters and their bandwidth is equal to the simulation frequency interval. Higher harmonic components can't be created by the multiplication within this simulation frequency range.

### B. Noise Modeling

The additive thermal noise is complex and is directly added to the useful transmitted signal in a transmission channel. The overall equivalent system noise temperature is recalculated [8] and expressed only in the transmission channel where the additive white Gaussian noise model AWGN is used. AWGN has a Gaussian distribution of amplitudes with a zero mean and a variance  $\sigma_{AWGN}^2$  directly equal to the additive noise power  $N$ . Since the baseband processing is used, the sampling frequency  $f_{sam}$  defines a noise bandwidth  $B_N$  of the transmission channel and its noise power is calculated as [9]

$$N = \sigma_{AWGN}^2 = N_0 \cdot B_N = N_0 \cdot f_{sam}, \quad (1)$$

where  $N_0$  is the additive noise power spectral density. Its flat frequency course secures that the additive noise power  $N$  is directly proportional to the noise bandwidth  $B_N$ . The impact of additive thermal noise in the transmission channel is related to the power of a modulated carrier wave and expressed via the ratio of  $C/N$  [9]

$$\frac{C}{N} = \frac{E_b}{N_0} \cdot \frac{f_b}{f_{sam}}, \quad (2)$$

where  $E_b/N_0$  defines the ratio of an energy per one information bit to the additive noise power spectral density.

The phase noise is produced in all system oscillators used

for the modulation, the demodulation and frequency transpositions. A signal of the harmonic oscillator degraded by the phase noise can be described by the equation (modified according to [10])

$$o_+(t) = O \cdot e^{j\psi(t)} \cdot e^{j\omega t} \cong O \cdot (1 + j\psi(t)) \cdot e^{j\omega t}, \quad (3)$$

where parameter  $\psi(t)$  represents time domain phase fluctuations.  $O$  is the signal amplitude and  $\omega$  denotes angular frequency of oscillations. The equation (3) expresses the oscillator analytical signal with one-sided spectrum (symbol + in a lower index). The last part of (3) shows, that phase fluctuations  $\psi(t)$  directly multiply the harmonic component, which arises from a simplification for sufficiently small values of  $\psi(t)$ . After removing the complex exponential from (3), one obtains the oscillator complex envelope that is directly used in simulations.

The phase noise modeling comes out from the frequency domain, where the asymptotic course  $L(f_m)$  is defined (SSB noise powers  $L$  on corresponding offset frequencies  $f_m$ , see Fig. 2). Between given values, the asymptotic course is linearly interpolated according to the sampling frequency  $f_{sam}$ . A logarithmic power scale is recalculated to the linear scale. A following operation is a randomization of the interpolated phase noise course by a sample by sample multiplication with a unity power AWGN vector. A frequency domain phase noise  $L(f_m)$  is transformed to the time domain course of phase fluctuations  $\psi(t)$  with a help of Inverse Fast Fourier Transform (IFFT) [10]. This procedure is used for each oscillator. The obtained course of phase fluctuations  $\psi(t)$  is substituted to the equation (3).

The great advantage of the described phase noise generation procedure is the possibility of a simulation of the arbitrary frequency domain phase noise course, which can be obtained by direct measurements.

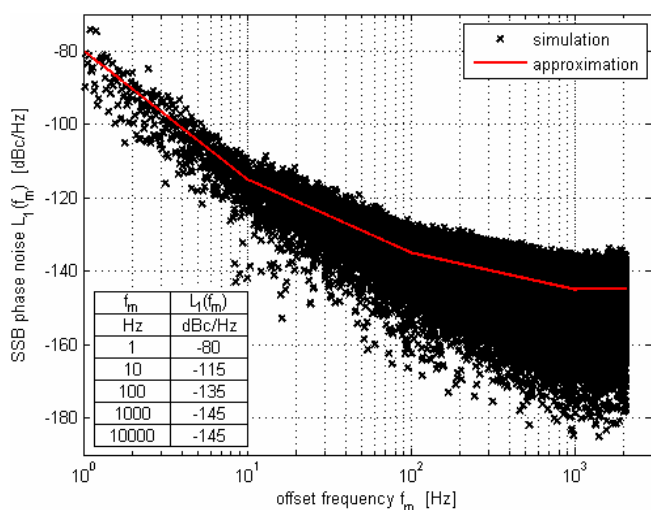


Fig. 2 An asymptotic phase noise course of modulator and demodulator oscillators

### III. SIMULATION RESULTS

The system model depicted in Fig. 1 is programmed in Matlab environment and put through simulations with settings described below. To cover the statistical character of noise processes, the random input data sequence is represented by a number of approximately  $17 \cdot 10^6$  bits. Three modulation techniques, differing in number of states, are used – BPSK, QPSK and 8-PSK.

#### A. Simulation Setup

Since one tries to simulate the impact of noise in low-rate data transmission systems, the data bit rate  $f_b$  is set to units of bit/s (see Tab. 1). To preserve the model simplicity, variables are in mutual multiples of power of 2.

Sampling frequencies  $f_{sam}$  for different values of bit rate  $f_b$  are given in Tab. 1. An integer multiple  $m = 128$ , which means that the number of samples per one bit period is identical for all values of  $f_b$ .

TABLE I  
 BASIC MODEL SETTINGS

| $f_b$     | b/s | 1     | 2     | 4        | 8        | 16       |
|-----------|-----|-------|-------|----------|----------|----------|
| $f_{sam}$ | Hz  | $2^8$ | $2^9$ | $2^{10}$ | $2^{11}$ | $2^{12}$ |
| BW        | Hz  | 4     | 8     | 15       | 32       | 64       |

Parameters of all oscillators are summarized in Tab. 2. The phase noise of modulator and demodulator oscillators is equally set in the frequency domain according to Fig. 2. These oscillators drive ideal phase lock loops deriving signals for mixers. The phase noise increases with frequency multiplication according to the relation [12]

$$L_2(f_m) = L_1(f_m) + 20 \cdot \log \frac{f_2}{f_1}, \quad (4)$$

where  $L_1(f_m)$  is the phase noise of the modulator oscillator,  $L_2(f_m)$  is the derived phase noise of up-mixer oscillator,  $f_2$  is the up-mixer oscillator frequency and  $f_1$  is the modulator oscillator frequency. The same method is used on the receiver side. There is also the possibility that phase noise courses of all oscillators can be set independently.

An AWGN transmission channel is modeled according to (2), where the ratio of  $E_b/N_0$  is chosen.

The receiver band-pass filter is modeled as an equivalent low-pass FIR filter with an order of 512. A roll-off factor is set to  $\beta = 1$ . The receiver filter bandwidth  $BW$  is derived from the value of the data bit rate  $f_b$  and is given in Tab. 1. The bandwidth of the transmitted signal is calculated according to the relation  $B = f_b(1+\beta)/2$  and the final filter bandwidth  $BW$  should be wider ( $BW > B$ ) to secure the proper signal detection.

A combination of RRC filters in the transmitter and the receiver represents the matched filter that maximizes the signal to noise ratio on the receiver. The cut-off frequency of the filter is equal to  $f_c = f_b/Mary$ , where the parameter  $Mary$  is derived from the number of modulation states (i.e.  $2^{Mary}$ ).

Orders of both RRC filters is evaluated according to the relation  $N_{RRCF} = 2^3 \cdot f_{sam} / ((1+\beta) \cdot f_C)$  [13].

TABLE II  
 PARAMETERS OF OSCILLATOR MODELS

|  |     | oscillators    |                |                |                |
|--|-----|----------------|----------------|----------------|----------------|
|  |     | O <sub>1</sub> | O <sub>2</sub> | O <sub>3</sub> | O <sub>4</sub> |
| output power*                                | W   | 1              | 1              | 1              | 1              |
| amplitude                                    | V   | 1              | 1              | 1              | 1              |
| frequency                                    | GHz | 0,01           | 10             | 10             | 0,01           |
| PN power*                                    | dBW | -75,5          | -15,7          | -15,4          | -75,2          |
| * power calculations related to 1Ω impedance |     |                |                |                |                |

### B. Constellation Diagrams

Simulation results represented as constellation diagrams are depicted in Fig. 3. As a representative outcome from three simulations, only results for QPSK modulation are shown, while the ratio of  $E_b/N_0 = 15$  dB. Diagrams demonstrate that AWGN causes the regular spreading of received symbols (see Fig. 3a)) around ideal states (marked by thick red squares). The phase noise PN changes the phase of the received symbol, while the amplitude (a distance from the origin) can be considered constant (see Fig. 3b)). An impact of both noise types combines in a general case with AWGN and PN (see Fig. 3b, marked by small black crosses).

It is obvious from Fig. 3, that the presence of phase noise is responsible for the error rate increase, which is more serious in systems with more modulation states (with the same phase noise power).

### C. BER Dependencies

Main simulation results are introduced by dependencies of BER on  $E_b/N_0$ . As a representative outcome, only the QPSK BER curves are chosen, the bit rate  $f_b$  is picked out from Tab. 1,  $E_b/N_0$  changes from 0 to 16 dB. Three simulation runs were performed – with an individual AWGN effect, with an individual PN effect and with a simultaneous impact of both AWGN and PN.

The individual influence of AWGN (see Fig. 4) confirms the correctness of the created model and of the used procedure. Simulation results are identical with the theoretical course of BER (generated from Matlab) for all bit rates. Certain deviations appear for higher values of  $E_b/N_0$  ( $E_b/N_0 > 9$  dB), where BER is very small and where only a few errors occur from the whole input set of bits (a small statistical credibility is given here).

Individual impact of phase noise on BER is constant with a dependency on  $E_b/N_0$  (see Fig. 5, dashed lines), but the BER value is influenced by the data bit rate  $f_b$ . BER is rising with increasing  $f_b$ .

The impact of a simultaneous incidence of both noise types can be divided into two regions (see Fig. 5, solid lines). For low rates of  $E_b/N_0$ , the final AWGN&PN BER is predominantly affected by the presence of AWGN. While for high rates of  $E_b/N_0$ , the final AWGN&PN BER is determined by the presence of PN. The final AWGN&PN BER course is

asymptotically nearing to the individual PN BER course (see Fig. 5).

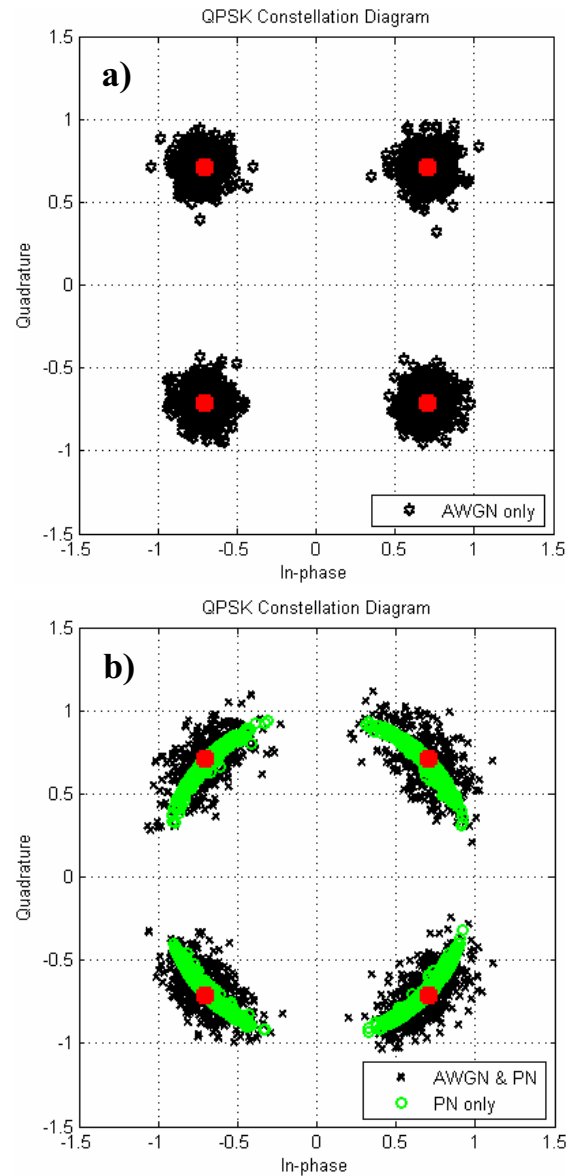


Fig. 3 Constellation diagrams for a QPSK system degraded by a) AWGN and b) PN and AWGN&PN;  $E_b/N_0 = 15$  dB

### D. Results Comparisons

If a certain noise power of phase noise of all oscillators is supposed, results for individual multi-state phase shift keying techniques can be compared.

In a case of two-state BPSK system, from a constellation diagram, the phase noise influences the phase, while the amplitude is considered the same. The BPSK detector is sensitive only on the In-phase channel, thus the phase noise has a little impact on the final error rate. No errors were observed for an individual presence of the phase noise, thus there is a very low probability that the received symbol jumps to the wrong semi-plane. This means that no individual PN

BER dependency on  $E_b/N_0$  can be depicted. In AWGN&PN BER dependencies for high rates of  $E_b/N_0$ , one can see a low indication of an asymptotic behavior (see Fig. 6). To confirm this phenomenon, very long simulation time should have to be set, which would take an extremely long simulation time.

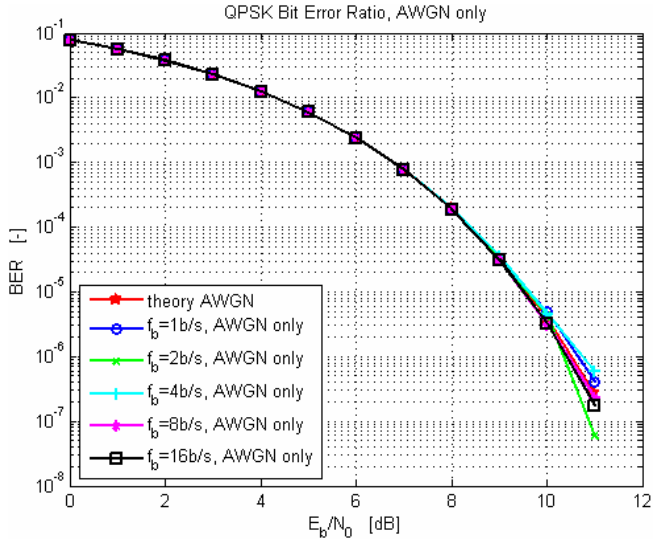


Fig. 4 QPSK dependencies of BER on  $E_b/N_0$ , for different bit rates  $f_b$ , with only an AWGN presence

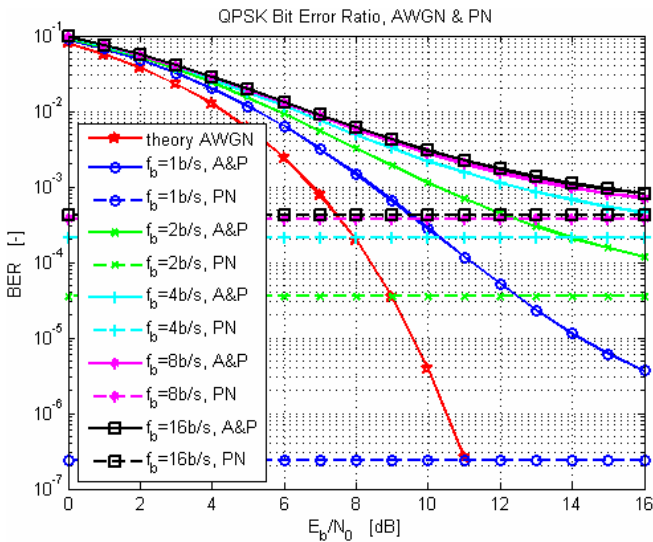


Fig. 5 QPSK dependencies of BER on  $E_b/N_0$ , for different bit rates  $f_b$ , with only a PN presence (PN) and with a simultaneous presence of AWGN and PN (A&P)

In a case of simulated multi-state QPSK and 8-PSK systems, constellation diagrams show analogous conclusions as for BPSK system. But since more states are deployed in a state plane, less space is reserved for each symbol and the probability of the error occurrence rises. Errors for an individual incidence of the phase noise occur and asymptotic nearing of AWGN&PN BER course to the individual PN BER course can be observed.

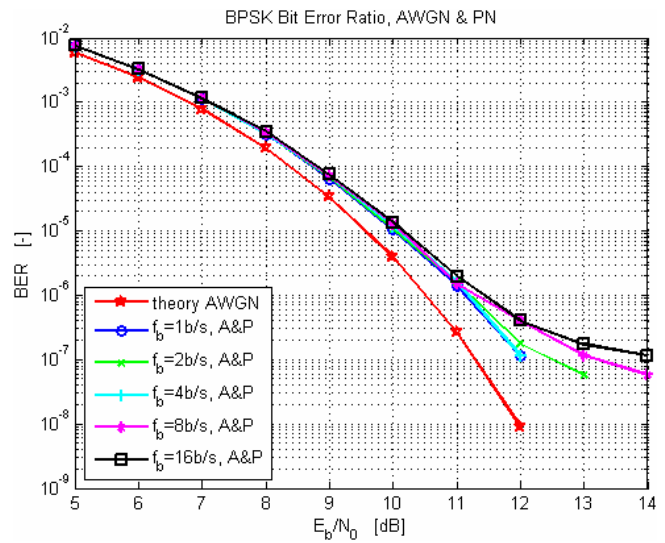


Fig. 6 A detail of BPSK dependencies of BER on  $E_b/N_0$ , for different bit rates  $f_b$ , with a simultaneous presence of AWGN and PN (A&P)

Generally, from constellation diagrams, the higher the number of modulation states is, the less space for right symbol detection is left and the higher the probability of errors appears. In BER courses displays, one can observe the raise of BER with increasing bit rate. This trend is more obvious with a raising number of modulation states. The higher the bit rate is, the lower the increase of BER can be observed. Thus, for high bit rates, it seems that BER is asymptotically nearing to some fix value of the error probability. Preliminary calculations show, that this asymptotic value of the error probability is directly tied with the total received phase noise power.

#### IV. CONCLUSION

The effect of the phase noise presence on bit error rate in the general multi-state phase shift keying satellite communication system is demonstrated via a system modeling in Matlab environment. The influence of the bit rate change is also investigated. A theoretical analysis and simulation results point out on a fact, that the phase noise primarily affects the quadrature branch. Thus the simple two-state BPSK modulation is rather phase noise immune, because it is insensitive on signals in a quadrature branch. With an increasing number of states in a state plane, the phase noise influence arises, a less space for proper symbol detection is left and the bit error ratio increases. For small ratios of  $E_b/N_0$ , the additive thermal noise plays the major role in a BER dependency. With an increasing ratio of  $E_b/N_0$ , the phase noise influence on BER is growing and finally, asymptotic nearing of the simultaneous additive and multiplicative noise BER course to the individual phase noise course is observed. The rise of user data bit rate causes the increase of BER. Simulation outcomes suggest, that a limit bit rate value exists, for which an increase of BER becomes negligible.

Our future work concentrates on rigorous statistical analysis of the phase noise behavior while the data bite rate is changed and phase noise courses of individual system oscillators are varied. Statistical results will help us to derive mathematical relations for a direct and faster evaluation of bit error rates in multi-state phase shift keying systems for the extraterrestrial low-rate data transmission.

#### ACKNOWLEDGMENT

This work has been supported by the Czech Science Foundation under the grant no. P102/10/1853 "Advanced Microwave Components for Satellite Communication Systems" and by the project CZ.1.07.2.3.00.20.0007 WICOMT of the operational programme Education for competitiveness.

#### REFERENCES

- [1] O. Baran, M. Kasal, "Modeling of the simultaneous influence of the thermal noise and the phase noise in space Communication systems," *Radioengineering*, 2010, vol. 19, no. 4, pp. 618-626. ISSN: 1210- 2512.
- [2] W. Jeong, J. Lee, D. Yoon, "New BER Expression of MPSK," *IEEE Transactions on Vehicular Technology*, May 2011, vol. 60, no. 4. pp. 1916-1924. ISSN: 0018-9545.
- [3] J. Lassing, E. G. Störm, E. Agrell, T. Ottosson, "Computation of the Exact Bit-Error Rate of Coherent M-ary PSK With Gray Code Bit Mapping," *IEEE Transactions on Communications*, November 2003, vol. 51, no. 11. pp. 1758-1760. ISSN: 0090-6778.
- [4] J. P. Lee, "Computation of the Bit Error Rate of Coherent M-ary PSK Gray Code Bit Mapping," *IEEE Transactions on Communications*, May 1986, vol. 34, no. 5. pp. 488-491. ISSN: 0090-6778.
- [5] S. Park, S. H. Cho, "Computing the Average Symbol Error Probability of the MPSK System Having Quadrature Error," *ETRI Journal*, vol. 28, no. 6, December 2006. pp. 793-795. ISSN: 1225-6463.
- [6] J. G. Proakis, *Digital Communications* (4th Edition), New York: McGraw-Hill, 2000, 1024 pages. ISBN 0-07-232111-3.
- [7] O. Baran, M. Kasal, P. Vágner, T. Urbanec, "Modeling of the Phase Noise Influence in the General M-PSK System," In *Proceedings of 5th International Conference on Recent Advances in Space Technologies*. Istanbul: 2011. pp. 393-398. ISBN: 978-1-4244-9615- 0.
- [8] O. Baran, M. Kasal, "Modeling of the Phase Noise in Space Communication Systems," *Radioengineering*, 2010, vol. 19, no. 1, pp. 141-148. ISSN: 1210- 2512.
- [9] K. Chang, *Encyclopedia of RF and Microwave Engineering*, New Jersey: John Wiley & Sons, 2005. ISBN 0-471-27053-9.
- [10] W. J. Riley, *Handbook of Frequency Stability Analysis*, Beaufort: Hamilton Technical Services, 2007, 158 pages. [Online] Cited 2012-03-07. Available at: <<http://www.stable32.com/Handbook.pdf>>.
- [11] A. Bar-Guy, Oscillator phase noise model, Matlab Central, An open exchange for the Matlab and Simulink user community. [Online] Cited 2012-03-07. Available at: <<http://www.mathworks.com/matlabcentral/fileexchange/8844>>.
- [12] D. Banerjee, *PLL Performance, Simulation, and Design* (4th Edition), August 2006. [Online] Cited 2012-03-07. Available at: <<http://www.national.com/appinfo/wireless/files/deansbook4.pdf>>.
- [13] Ansoft Designer/Nexxim, version 3.0.0, 2006. Ansoft Designer System Simulator Help.